Field-induced exchange effects in (Cd,Mn)Te and (Cd,Mn)Se from photoluminescence measurements

D. Heiman and P. Becla

Francis Bitter National Magnet Laboratory, Massachusetts Institute of Technology, Cambridge, Massachusetts 02139

R. Kershaw, D. Ridgley, K. Dwight, and A. Wold

Department of Chemistry, Brown University, Providence, Rhode Island 02912

R. R. Galazka

Institute of Physics, Polish Academy of Sciences, Warsaw, Poland

(Received 24 March 1986)

Photoluminescence measurements are made on the semimagnetic semiconductors $Cd_{1-x}Mn_xTe$ and $Cd_{1-x}Mn_xSe$ for $0 < x \leq 0.15$. Large energy shifts (~ 50 meV) of the exciton recombination peaks and large optical polarizations ($\sim 100\%$) are produced by applying a magnetic field. This study examines changes in luminescence using magnetic fields up to $B = 15$ T and at temperatures between $T = 1.5$ and 60 K. When viewed along the direction of the field (Faraday geometry), the luminescence due to both exciton recombination and impurity-related transitions becomes circularly polarized. At $T = 2$ K the polarization shows saturation at only 0.5 T. This low saturation field results from the large internal exchange field which produces large spin Zeeman splitting of the bands. We found that the polarization gives a quantitative measure of the exchange effects *even when the luminescence features are broader than the splittings*. In the Voigt geometry (luminescence observed perpendicular to the magnetic field), the linear polarization gives information on the *orbital* part of the wave functions of the recombining carriers. Differences in the polarization of the two exciton-related peaks in the (Cd,Mn)Te spectra indicate that one peak arises from an acceptor-bound exciton complex and the second to a simple electron-hole exciton. The latter is attributed to a trapped exciton. With increasing magnetic field, both the (Cd,Mn)Te and (Cd,Mn)Se spectra show splittings of the bound exciton related peaks. At low fields the low-energy feature dominates while at high fields the higher-energy feature is dominant. This is attributed to a field-induced instability of the binding of the exciton to the impurity, resulting from the exchange interaction and Pauli exclusion. At high magnetic fields and low temperature the energy of the exciton peak shows a step in the field-tuning curve. This step reflects a transition of the antiferromagnetically coupled nearest-neighbor manganese ion pair. A value of $J/k = -8.4$ K is determined for the exchange constant. Finally, the luminescence spectra indicate that samples grown by liquid-phase epitaxy and the traveling-solvent method have much higher purity than Bridgman-grown materials. The manganese concentrations in (Cd,Mn)Te are determined from the energies of the exciton luminescence peaks.

I. INTRODUCTION

In semimagnetic semiconductors (SMSC's) the exchange interaction between the spins of carriers and localized magnetic ions gives rise to large Zeeman splittings of energy bands[1,2] and to magnetic polaron effects.[3] An applied magnetic field has been shown to produce large Faraday rotation,[2] strongly tunable bands observed in reflectivity[4] and photoluminescence,[5] and enhanced Landé g factors.[6] In addition to enhanced magnetic field effects, bound magnetic polarons (BMP's) produce sizable internal exchange fields when carriers become localized. This has been observed in bound-exciton luminescence[7] and spin-flip Raman scattering.[8,6] Following these observations of BMP's, theoretical models were developed using classical macroscopic approaches[9,10] and a microscopic statistical mechanical model.[6]

Photoluminescence (PL) is a simple and valuable technique for measuring some of these exchange effects. Many studies have been made on (Cd,Mn)Te and

(Cd,Mn)Se since they produce strong PL associated with band-edge states. Magnetic field tuning of PL due to exciton recombination has been reported for the (Cd,Mn)Te spectra by Komarov et al.,[5] Planel et al.,[11] and Ryabchenko et al.[12] Tuning of the (Cd,Mn)Se spectra was described by Gubarev and Shepel,[13] and Heiman.[14] (PL from recombination involving Mn^{2+} levels was studied by Vecchi et al.[15] and Becker et al.[16])

The importance of BMP effects in SMSC's was first discussed by Golnik et al.[17]—they observed large temperature-dependent shifts of acceptor-bound exciton recombination PL from (Cd,Mn)Te. Subsequently, quantitative measurements of acceptor BMP energies were determined from time-resolved spectroscopy of donor-acceptor pair PL in (Cd,Mn)Te by Nhung et al.[18] Shortly after, a bottleneck in the BMP formation was observed by Heiman et al.[19] using field-induced polarization of PL in (Cd,Mn)Se. A thorough study of magnetic polaron effects on exciton PL of (Cd,Mn)Te was made by Golnik, Ginter, and Gaj.[20] These observations led to qualitative calcula-

tions of acceptor-bound exciton-polaron energies made by Nhung *et al.*[18] and Warnock and Wolff.[21] It was later shown that BMP energies of bound excitons can be measured in a more straightforward way via excitation spectroscopy as demonstrated by Warnock *et al.*[22] on (Cd,Mn)Te and (Cd,Mn)Se. Finally, the polaron formation time of excitons has been measured by Harris and Nurmikko.[23] In addition to this work, Zayhowski *et al.*[24] used picosecond time-resolved PL to measure polaron formation times of excitons, and concludes that the electron carries Mn^{2+} spin magnetization to the center of the polaron where the hole is localized.[25]

This paper describes results of PL from $Cd_{1-x}Mn_xTe$ and $Cd_{1-x}Mn_xSe$, $x \sim 10^{-1}$, as a function of temperature and applied magnetic field. In Sec. II we compare PL spectra of (Cd,Mn)Te samples grown by various methods and use the PL energy to determine the manganese concentration x. Section III describes the magnetic-field-induced polarization of PL in both Faraday (B parallel to PL) and Voigt (B perpendicular to PL) configurations. The PL becomes circularly polarized in the Faraday geometry resulting from *spin* alignment of the recombining carriers. On the other hand, the *orbital* contributions to the carrier wave functions produce PL linearly polarized perpendicular to the field (Voigt geometry). The outstanding feature of this technique is that it provides quantitative information on exchange *even when the PL spectral width is wide compared to the field shift*. In Sec. IV we show results of field-induced transitions of excitons bound to donors and acceptors; when the magnetic energy overcomes the binding energy, the exciton becomes free of the impurity trap. Last, Sec. V discusses a field-induced transition of a pair of manganese ions on nearest-neighbor sites. Here, since the field tuning of exciton PL is largely governed by the magnetization, a step is seen in the tuning curve when the antiferromagnetic exchange energy of a nearest-neighbor pair of magnetic ions is overcome by the magnetic energy.

II. EXPERIMENT

Samples of (Cd,Mn)Se were grown by the Bridgman method[26] at Brown University. They were not intentionally doped but had a large range of carrier concentrations. Unannealed samples showed large room-temperature resistivities ($> 10^6 \Omega$ —cm) because of donor-acceptor compensation. Annealing produced low-resistivity material with room-temperature electron concentrations $N_D - N_A \sim 10^{16}-10^{17}$ cm^{-3}, where the concentrations of donor and acceptor impurities, N_D and N_A, are probably of the same order. The manganese concentrations of the selenium-base materials were determined from magnetization measurements at room temperature.

(Cd,Mn)Te samples[27] were grown by the Bridgman technique, liquid-phase epitaxy (LPE) and by the traveling-solvent method (TSM).[28] Comparison of Bridgman and TSM samples is shown in Fig. 1(a). PL from the Bridgman sample is dominated by a feature attributed to recombination of excitons bound to neutral acceptors (labeled L 1), while the TSM sample shows a narrower peak (3 versus 8 meV) arising from free or self-trapped exciton
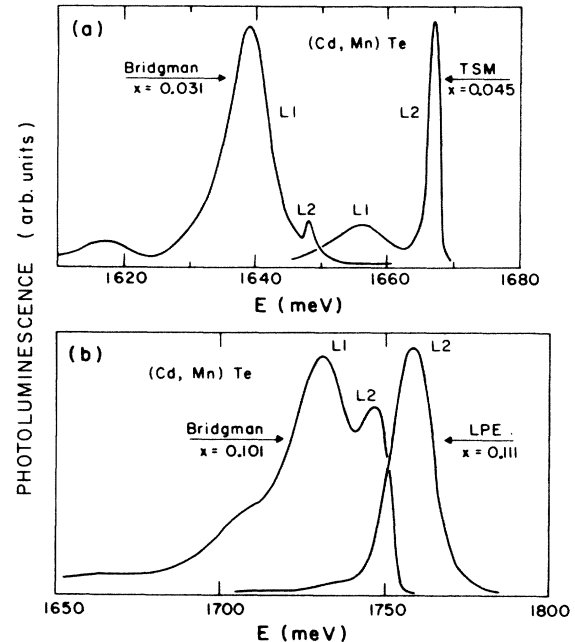

FIG. 1. Photoluminescence intensity versus photon energy for $Cd_{1-x}Mn_xTe$ grown by different methods, and at $T = 2$ K. The peaks labeled L 1 and L 2 refer to recombination luminescence of excitons. In (a) the curve on the left was obtained from a sample grown by the Bridgman method, and the curve on the right was from a sample grown by the traveling solvent method (TSM). In (b) are spectra from Bridgman and liquid-phase-epitaxy (LPE) growth techniques.

recombination (labeled L 2). (Reflectivity measurements on low-x samples gave nearly the same exciton energy as the L 2 line.) Thus, the TSM sample has a lower impurity concentration and we estimate the total impurity concentration at $N_D + N_A \sim 10^{16}$ cm^{-3}, while $N_D + N_A \sim 10^{16}-10^{17}$ cm^{-3} for the Bridgman-grown materials. PL spectra for an LPE sample are shown in Fig. 1(b) along with a bulk-grown sample. The LPE spectra showed no L 1 bound-exciton PL, indicating total impurity concentrations lower than either TSM- or Bridgman-grown materials. The higher purities obtained by TSM and LPE growth techniques are due to the purifying process of the liquid tellurium.

The manganese concentrations, x, of the $Cd_{1-x}Mn_xTe$ samples were determined from the energies, E, of exciton-recombination PL and free-exciton (FX) reflectivity. A simple fiber-optic setup[29] was used for measuring E while the samples were immersed in a liquid-helium storage dewar. In Bridgman-grown samples two PL features were observed below the free-exciton energy and have been referred to as L 1 and L 2 by Golnik, Ginter and Gaj.[20] They assigned the L 1 peak to recombination of excitons bound to neural acceptors. For $x < 0.1$, E_{FX} determined from reflectivity coincided closely with the L 2 peak. We determined empirical relations for $E(x)$ by fitting their data. At $T = 4$ K

$$E_{FX} = 1597.6 + 1564x \text{ meV for } 0 < x \le 0.2 \ ,$$

$$E_{L1} = 1588.8 + 1440x \text{ meV for } 0 < x \le 0.1 \ ,$$

and

$$E_{L2} = 1604.7 + 1397x \text{ meV for } 0.05 \le x \le 0.2$$

$$= 1575 + 1536x \text{ meV for } 0.2 \le x \le 0.4 \ ,$$

for the free-exciton and $L1$ and $L2$ PL lines. (For $x \le 0.1$ this compares favorably with $E_{FX} = 1595 + 1587x$ meV measured by Twardowski, Nawrocki, and Ginter.[30]) We estimate an absolute accuracy in x of ± 0.003 based on their data and a precision of ± 0.0003. We used this method to determine the composition profile in 2.5-cm-diameter, $x = 0.2$ boules. Typical longitudinal variations in x were less than ± 0.001, except in the outer edges (≤ 1 mm) where x deviated by two or three times this value. For samples with $0 < x \le 0.7$, x can also be determined from E_{FX} via reflectivity measurements. At $T = 10$ K, Stankiewicz, Bottka, and Giriat's data[31] give $E_{FX} = 1588 + 1584x$. Lee and Ramdas[32] find

$$E_{FX} = 1595 + 1592x \text{ meV at } T = 10 \text{ K}$$

and

$$E_{FX} = 1586 + 1501x \text{ at } T = 80 \text{ K} \ .$$

The manganese concentration in (Cd,Mn)Se $0 < x \le 0.4$, can likewise be determined from reflectivity using the results of Stankiewicz,[33]

$$E_{FX} = 1820 + 1490x \text{ at } T = 10 \text{ K}$$

and

$$E_{FX} = 1791 + 1440x \text{ at } T = 100 \text{ K} \ .$$

In these and the following PL experiments, optical excitation was provided by a He-Ne laser. When not using the fiber-optic setup,[29] the laser was focused by a cylindrical lens to intensities of $10^{-2} - 10^{0}$ W/cm^2 and samples were mounted in a variable-temperature liquid-helium dewar. Below $T = 2$ K they were in contact with superfluid helium, and in flowing helium gas for $T > 4$ K. A Bitter magnet with radial access provided fields to $B = 10$ T in a vertical direction. The sample surface was placed either perpendicular or parallel to the field for Faraday and Voigt configurations, respectively. In the Faraday configuration, the excitation and PL light were turned 90° to the horizontal with a small mirror at 45° placed directly above the sample. The PL polarization was analyzed with quarter-wave and linear Polaroid-type polarizers.

III. MAGNETIC-FIELD-INDUCED POLARIZATION OF LUMINESCENCE

A. Faraday geometry

In a previous communication we demonstrated that weak fields applied to (Cd,Mn)Se at low temperatures produce strong circular polarization in the Faraday configuration (field parallel to the direction of PL).[19] This can be described by the alignment of hole BMP's in a magnetic
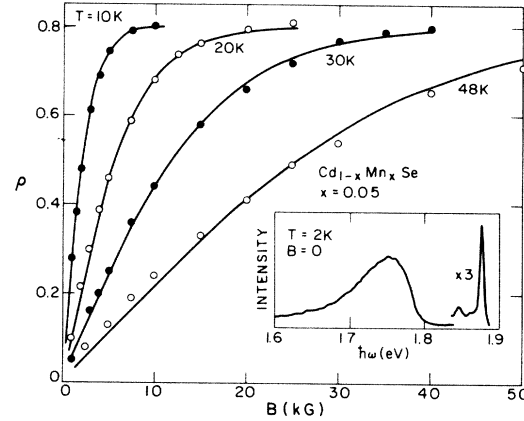
FIG. 2. Polarization of luminescence in the Faraday configuration ρ versus applied field B for the donor-acceptor pair band (1760 MeV) of $Cd_{1-x}Mn_xSe$, $x = 0.05$, for various temperatures T. The solid curves represent Eq. (1) with p fit at each temperature. The inset shows the photoluminescence spectrum at $T = 2$ K. The field was applied along the c axis of the sample.

field. The s-d exchange interaction thus produces an effective magnetic moment for the acceptor-bound hole that can be as large as 50 Bohr magnetons.

Figure 2 shows the polarization, defined by $\rho_F \equiv (I_+ - I_-)/(I_+ + I_-)$, where I_+ and I_- refer to the light intensities for right and left circular polarizations, respectively. These results are for the donor-to-acceptor pair (DAP) recombination in $Cd_{1-x}Mn_xSe$, $x = 0.05$. Qualitatively similar results were seen for the exciton luminescence in $x = 0.05$ and for both DAP and exciton luminescence in $x = 0.1$ samples. The polarization curves rise linearly from $B = 0$ and saturate at 80% polarization. For increasing temperature the field needed for saturation increases. The linear rise followed by saturation is similar to the paramagnetic magnetization, except the field scale for polarization is an order of magnitude smaller. The smaller field scale for the polarization occurs because the *magnetization* arises from $g = 2$ Mn^{2+}-ion spins aligning in the field B. On the other hand, the *polarization* is due to the alignment of the hole spin in the *enhanced* exchange field. Or equivalently, the applied field aligns the *enhanced* hole spin, which has an aligned spin cloud of magnetic ions.

The data were fit to

$$\rho_F = \rho_0 \tanh(p\mu_B B/kT) \ , \tag{1}$$

where ρ_0 is a temperature-independent constant and p is the effective number of Bohr magnetons (μ_B) at a given temperature. Figure 3 shows how p varies with temperature. The moment reaches a maximum of $p \sim 50$ at $T = 12$ K. For larger temperatures the moment decreases as T^{-1}. This is caused by the decreasing exchange field when the temperature increases, due to lower magnetic susceptibility. Below $T = 10$ K the moment also decreases, where $p \sim T$. This cannot be explained by a thermal equilibrium model and we have described it using
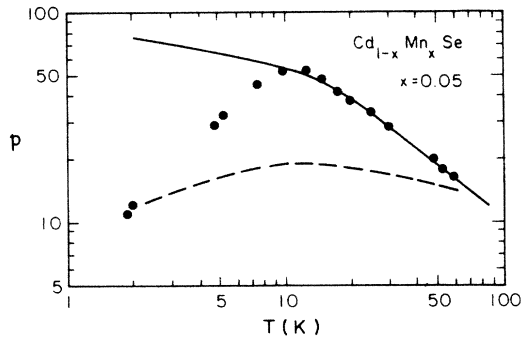
FIG. 3. Effective number of Bohr magnetons p versus temperature T from polarized donor-acceptor pair luminescence of $Cd_{1-x}Mn_xSe$, $x = 0.05$. The solid curve is the theory of Eq. (2) with $a_0 = 8.5$ Å. The dashed curve was obtained by limiting the number of ions to $N = 70$.

FIG. 4. Photoluminescence intensity versus photon energy for $Cd_{1-x}Mn_xTe$, $x = 0.10$. A magnetic field of $B = 5$ KG was applied in the Voigt geometry ($\vec{B}$ perpendicular to luminescence direction), and the linear polarization ($\hat{e}$) was selected either parallel or perpendicular to the field. The lattice temperature was $T = 2$ K, and $L\,1$ and $L\,2$ are explained in the text.

a model with a spin-diffusion bottleneck.[19]

The expected optical polarization is calculated by determining the acceptor spin polarization using a statistical mechanical model.[6] We assume that the acceptor state is made from the upper valence band ($m_j = \frac{3}{2}$), having a wave function $(\pi a_0^3)^{-1/2}e^{-r/a_0}$. The moment is given by[19]

$$p = 10g\bar{x}\int_0^\infty r^2 dr\, B_{5/2}(5JN_0 e^{-2r/a_0}/4\pi a_0^2 k(T + T_0))\ ,$$

(2)

where $g = 2$, $\bar{x} = 0.03$,[34] $JN_0 = (\alpha - \beta)N_0 = 1110$ meV,[35] $T_0 = 1.5$ K,[34] $B_{5/2}$ is the Brillouin function, and a_0 is the acceptor Bohr radius which is used as the fitting parameter. The best fit to the data for $T > 12$ K is shown by the curve in Fig. 3 with $a_0 = 8.5$ Å. The value of a_0 is consistent with that for acceptors in CdSe. Although we have taken $\bar{x}$ and T_0 as constants, they both vary with temperature. In general, $\bar{x} \rightarrow x$ and $T_0 \rightarrow T_c$ (Curie-Weiss temperature) by about $T = 40$ K. We estimate an error of $\sim 30\%$ in p at $T = 40$ K.

In view of the above, our model of the hole BMP describes the polarization data for $T > 12$ K. Below this temperature, the data can be fit by assuming that the spin magnetization is not allowed to propagate freely at low temperature. We assume that within a small volume the total magnetization is conserved; the hole redistributes the magnetic ion spins so that they are aligned near the center of the Bohr orbit at the expense of those farther out. At $T = 2$ K the number of ions needed to fit the data is $N = 70$. At $T = 5$ K, $N = 250$.

It is important to note that exchange-enhanced effects can be observed via polarization even when the spectral lines are very broad. This has been observed here for donor-acceptor pair PL,[19] and in superlattice PL.[36]

B. Voigt geometry

In the preceding subsection we used the Faraday configuration to measure the spin moment of the polaron. Now we use the fact that the linear polarization in the Voigt configuration (B field perpendicular to the lumines-
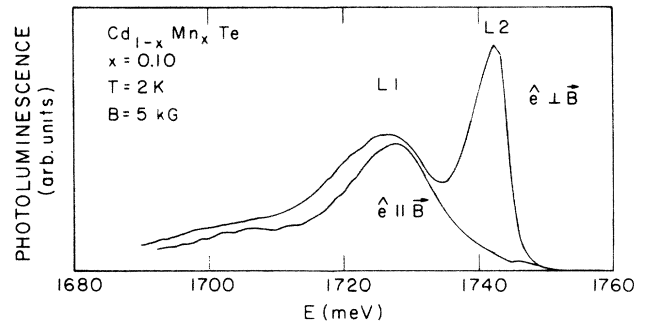
cence direction) give information on the orbital part of the BMP wave functions.

Figure 4 shows the luminescence from (Cd,Mn)Te, $x = 0.10$, $T = 2$ K with a magnetic field of $B = 5$ kG. The low-energy peak ($L\,1$) is weakly polarized while the high-energy peak ($L\,2$) is strongly polarized. Figure 5 is a plot of the linear polarization $\rho_v \equiv (I_x - I_z)/(I_x + I_z)$ as a function of temperature T and applied field B, where I_x
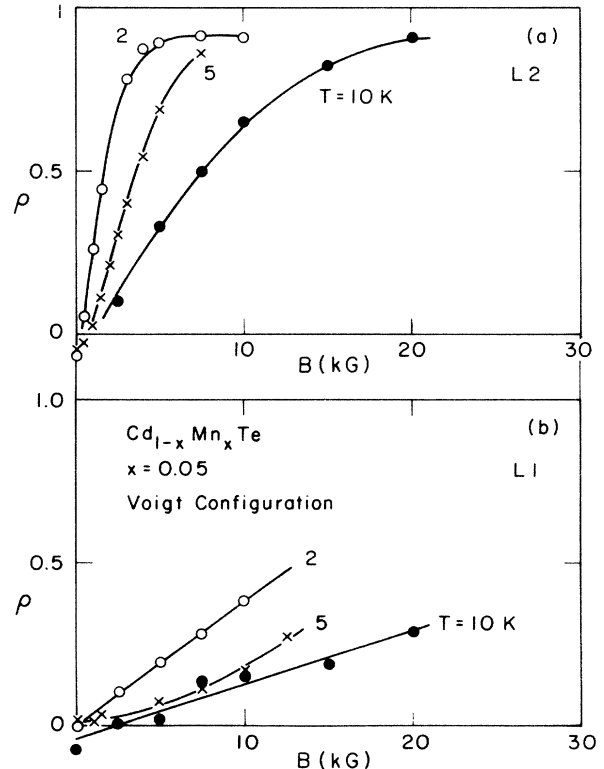

FIG. 5. Linear polarization of luminescence in the Voigt configuration ρ versus applied magnetic field B for $Cd_{1-x}Mn_xTe$, $x = 0.05$, at various temperatures T. Results for the $L\,2$ line are shown in (a) and for the $L\,1$ line in (b). The solid curves were drawn to aid the eye.

and I_z are the intensities for linear polarizations perpendicular and parallel to the field ($\mathbf{B}||\hat{z}$). The line $L2$ polarizes quickly with increasing B and reaches almost total polarization ($\rho_v \sim 1$). On the other hand, the line $L1$ polarizes slowly and is only observed for $\rho_v < \frac{1}{2}$.

The $L1$ peak has been identified[11] as an acceptor-bound exciton, (A^0X). It has two holes with the two available states $m_j = -\frac{3}{2}$ and $m_j = -\frac{1}{2}$ (z component of angular momentum). The total hole wave function is made from the product of

$$\frac{1}{\sqrt{2}}|(x-iy)\downarrow\rangle \text{ for } m_j = -\frac{3}{2}$$

and

$$\frac{1}{\sqrt{6}}|(x-iy)\uparrow + 2z\downarrow\rangle \text{ for } m_j = -\frac{1}{2} .$$

Thus the polarization is small, $|\rho| \sim 10^{-1}$, which is consistent with the data for the $L1$ peak. On the other hand, the $L2$ peak has $\rho_v \rightarrow 1$, indicating that the hole giving rise to the recombination luminescence is predominantly an $m_j = -\frac{3}{2}$ state. This gives additional evidence that $L2$ is due to a simple electron-hole pair (exciton). Since it also shows a temperature-dependent energy shift, a BMP signature, it may be a trapped exciton, as suggested previously.[20] We observe similar behavior in (Cd,Mn)Te with $x = 0.05$ and 0.15.

IV. FIELD-INDUCED EXCITON TRANSITIONS

A. Donor-bound exciton

(Cd,Mn)Se commonly shows n-type conductivity, which leads to strong recombination PL of excitons bound to neutral donors (D^0,X).[37] The complex, shown schematically in Fig. 6(a), has two weakly-bound electrons occupying an s-like orbital around the positive impurity center. These electrons screen out the positive center from the mobile hole which lies farther out in an annular shell (when not localized). When no external field is applied and the BMP effect for electrons is small, the electron spins will be paired antiparallel in an $S=0$ singlet state. At some applied magnetic field B_c one of the electron spins can lower its energy by going to a larger orbital or by autoionizing. This is shown in Fig. 6(b) and has also been discussed by Bryja and Gaj.[38] The spin-up state of the bound orbital flips its spin and makes a transition to the free state when $B > B_c$, shown by the heavy line. Since the electron in the free state has a larger overlap with the hole, the PL is predominately at the higher energy. We note that the state labeled "free" may actually be a loosely-bound orbital such as an $n=2$ hydrogenic state.

This transition is seen in Fig. 7 which shows the field dependence of the exciton PL spectrum of (Cd,Mn)Se, $x = 0.05$. The lowest trace at $B = 0$ has a single peak at $E = 1881$ meV. At small fields another peak becomes apparent at *higher* energy. For increasing B the higher-E peak eventually dominates, while the lower-E peak vanishes. A transition field B_c can be defined by equating the magnetic energy to the energy difference between the two states ΔE,
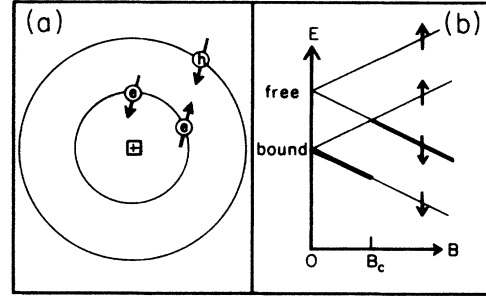

FIG. 6. Donor-bound exciton complex. In (a) is a schematic representation of paired electron spins orbiting a positive impurity center. The spin-down hole ($m_j = -\frac{3}{2}$) recombines with the spin-down electron ($m_j = -\frac{1}{2}$). In (b) is a plot of the Zeeman splitting for the bound electron shown in (a) and an unbound electron. Above B_c the hole recombines with the spin-down free electron.

$$B_c = \Delta E / \tilde{g}_e \mu_B ,$$

where $\tilde{g}_e$ is the effective g value for the electron. Using[6] $\tilde{g}_e = 35\bar{x}(\alpha N_0)g_{Mn}/12k(T+T_0)$, $\bar{x} = 0.03$, $\alpha N_0 = 260$ meV,[34] $g_{Mn} = 2$, and $T_0 = 1.5$ K,[34] we get $\tilde{g}_e = 150$. For $\Delta E = 4.6$ meV, the transition field is $B_c = 0.5$ T. At this
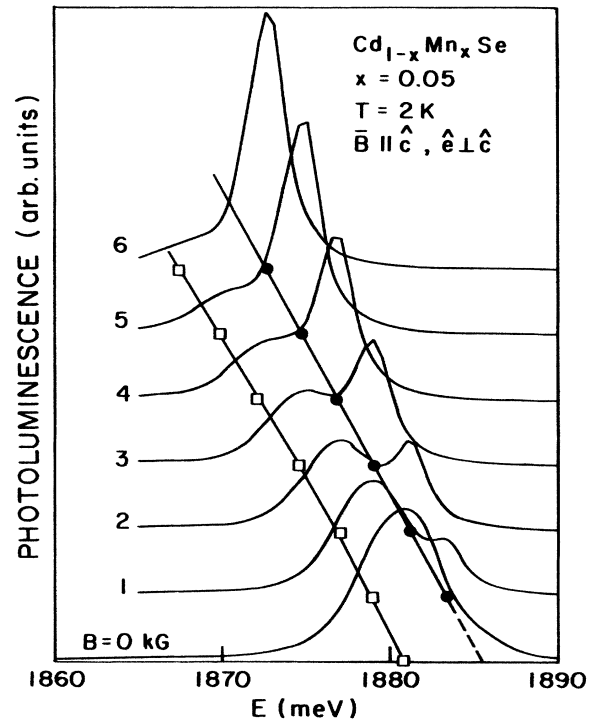

FIG. 7. Photoluminescence intensity versus photon energy for $Cd_{1-x}Mn_xSe$, $x = 0.05$, for various applied magnetic fields B. Solid curves were drawn through the open squares which represent the energy of the lower-energy peak, while the solid circles denote the high-energy peak. The lattice temperature was $T = 2$ K, the field was applied parallel to the c axis of the sample and the luminescence polarization was selected perpendicular to the c axis.

field the high-E peak is clearly dominant. At a higher temperature, $T = 10$ K, two things are different from the previous data: Higher fields are needed to produce the transition to the higher-E peak, and the field tuning of the peaks is slower. Both effects are due to a reduction in the effective g factor at higher T. For this temperature $\tilde{g}_e = 46$ and $B_c = 1.7$ T. We also note that BMP corrections of ~ 1 meV should reduce ΔE and consequently lower B_c by $\sim 20\%$.

B. Acceptor-bound excitons

The PL spectrum of low-x ($\sim 10^{-1}$) (Cd,Mn)Te usually has a strong component due to recombination of excitons bound to acceptor impurities because of its p-type character. This complex, shown schematically in the inset of Fig. 8, contains two holes in an orbit around the negatively charged impurity center and a loosely-bound electron in a larger orbit. The constraint of having a symmetric spatial part of the two-hole wave function requires that the total magnitude of angular momentum of the two holes be $M_J = 0$ or 2.[20] At low temperature the internal field of the BMP rules out the opposed spin states $(m_j^1, m_j^2) = (-\frac{3}{2}, +\frac{3}{2})$ and $(-\frac{1}{2}, +\frac{1}{2})$, leaving only the
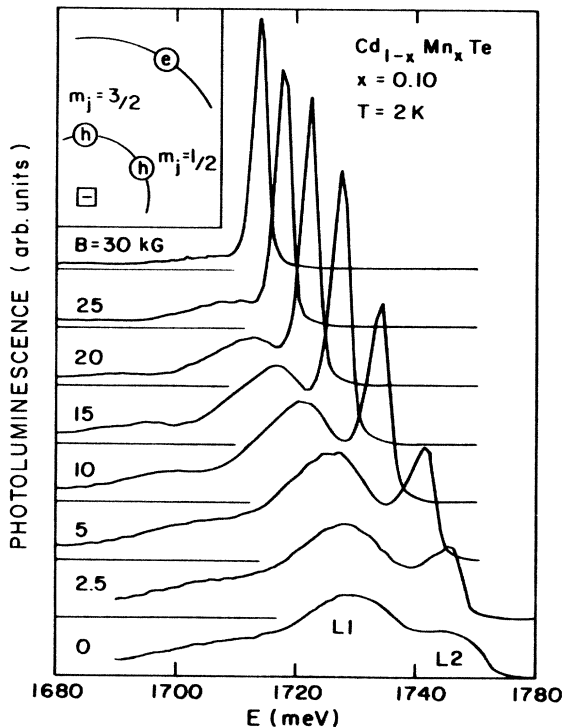

FIG. 8. Photoluminescence intensity versus photon energy for $Cd_{1-x}M_xTe$, $x = 0.10$, for various applied magnetic fields B. The peaks labeled $L1$ and $L2$ are explained in the text and the lattice temperature was $T = 2$ K. The inset shows schematically the acceptor-bound exciton complex with the square as the negatively charged impurity center surrounded by two holes with z components of angular momentum $m_j = \frac{1}{2}$ and $m_j = \frac{3}{2}$, and a loosely bound electron in a larger orbit.

$(-\frac{3}{2}, -\frac{1}{2})$ combination. (The BMP field also lifts the degeneracy of the $m_j = -\frac{1}{2}$ and $-\frac{3}{2}$ hole.) With the addition of a large enough external magnetic field the $m_j = -\frac{1}{2}$ hole can lower its energy by making a transition to an $m_j = -\frac{3}{2}$ state and large spatial orbit, effectively becoming ionized. A similar mechanism was discussed previously by Planel, Gaj, and Benoit à la Guillaume[11] and Nhung *et al.*[18] Figure 8 shows the PL spectrum of (Cd,Mn)Te, $x = 0.1$ as a function of applied field. The lower-energy peak gets weaker for increasing field similar to the (D^0, X) PL in (Cd,Mn)Se spectra. We take this as evidence for a transition from an $m_j = -\frac{1}{2}$ to $-\frac{3}{2}$ hole state while the exciton effectively loses its binding to the acceptor impurity. The value of the external field at the transition was not determined since the biasing field of the BMP is not accurately known. It was noted that the transition at higher temperatures required only slightly higher applied fields. For these reasons, we will not make a quantitative comparison.

V. MANGANESE PAIR TRANSITION

A pair of Mn^{2+} ions ($S = \frac{5}{2}$, $g = 2$) on nearest-neighbor sites has an antiferromagnetic exchange coupling energy J. At low temperatures $T \ll J/k_B$, this interaction results in total spin of $S_T = 0$ for such a pair. In a magnetic field B the pair energy is

$$E = -J[S_T(S_T + 1) - \frac{35}{2}] - g\mu_B M_s B ,$$

where $S_T = 1,2,3,4,5$ and $M_s = -S_T, -S_T + 1, \ldots, S_T$. The last term in the energy (Zeeman term) leads to energy-level crossing at finite B. Specifically, in strong fields (usually $B \gtrsim 10$ T) the state with $S_T = 0$ is no longer the ground state. The first switch in the ground state occurs when the last term makes $S_T = 1$ the lowest energy. The magnetic transition from $S_T = 0$ to 1 occurs when $g\mu_B B_0 = 2|J|$ and results in a steplike increase in the magnetization at B_0.[39,40] Additional magnetization steps occur at higher fields, corresponding to changes of S_T of the ground state. In total, there are five steps, up to $S_T = 5$. The relative magnitude of the step depends on x and is comparatively large at $x \sim 0.05$.[39] Observation of this step at $g\mu_B B = 2|J|$ provides a direct means to measure J. This has been used to determine J from high-field magnetization measurements.[39] Other experiments that measure quantities which are related to the magnetization can also show this step, such as exciton reflectivity, magnetoresistance, specific heat, exciton luminescence, Faraday rotation, and spin-flip Raman scattering. So far, $2|J|$ has been measured by magnetization,[39,41] reflectivity,[40,42] magnetoresistance,[43] luminescence,[29] neutron scattering,[44] and Faraday rotation[45] experiments.

To interpret exciton PL experiments, we express the primary exchange contribution to the exciton energy as[14]

$$E_x = E_0(B) - \frac{(\alpha - \beta)N_0}{2g\mu_B N_0} M(B) ,$$

where $M(B)$ is the magnetization. $E_0(B)$ is the energy of the recombining exciton in the absence of the exchange interaction and is in general somewhat field dependent. The
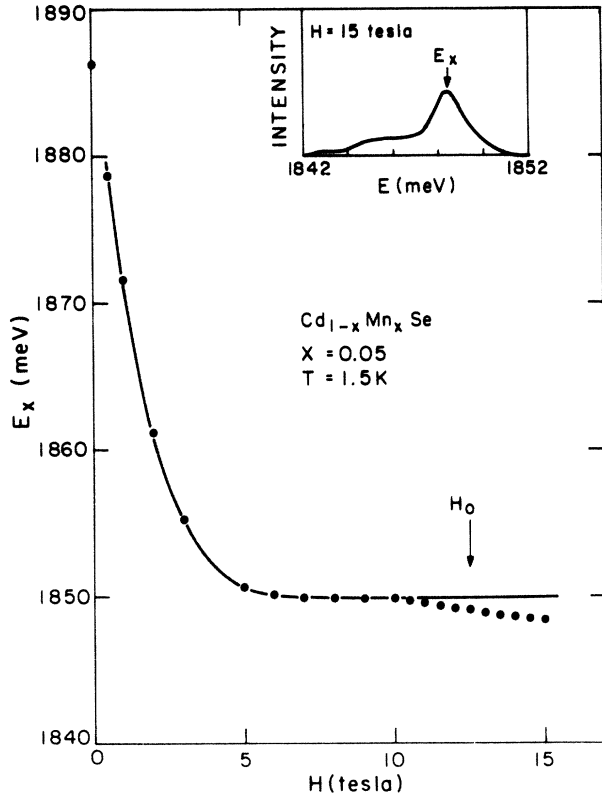
FIG. 9. Photon energy of exciton photoluminescence spectral peak E_x versus applied magnetic field H for $Cd_{1-x}Mn_xSe$, $x = 0.05$, and temperature $T = 1.5$ K, from Ref. 9. The solid curve was drawn to aid the eye. The arrow at $H_0 = 12.5$ T is drawn at the center of the step in the tuning curve. The inset shows the photoluminescence spectrum at $H = 15$ T.

FIG. 10. Photon energy of exciton photoluminescence spectral peak E versus applied magnetic field B for $Cd_{1-x}Mn_xTe$, $x = 0.05$ and temperature $T = 1.6$ K. The closed circles represent strong intensity peaks and the open circles are for weaker peaks. The solid and dashed curves were drawn through the data for clarity.

magnetization arises from both the external field and the internal or local (BMP) magnetization. When E_0 is weakly dependent on B and BMP effects are small, then $E_x(B)$ varies linearly with $M(B)$ and will reflect the pair transition step. Figures 9 and 10 show high-field exciton luminescence of (Cd,Mn)Se and (Cd,Mn)Te, respectively. The step is observed for (Cd,Mn)Se at $B_0 = 12.5 \pm 0.5$ T, which results in $J/k_B = -8.4 \pm 0.7$ K. This value agrees with those obtained from direct magnetization[39] and reflectivity.[40] The apparent relative magnitude of the step is 3% and is expected to be 8%.[39] This reduction arises from a background increase in $E_0(B)$ caused by diamagnetic and $n = 0$ Landau level effects;[46] $E_0(B)$ increases quadratically with increasing field at first, then eventually approaches the linear Landau level at higher fields. This increase is more severe in materials with smaller effective masses (smaller band gap). In the (Cd,Mn)Te spectra, shown in Fig. 10, this completely obscures the first step. On the other hand, in large effective-mass materials the luminescence technique may not be accurate because of the strong internal exchange field of the BMP. This additional biasing field of the BMP is difficult to quantify.
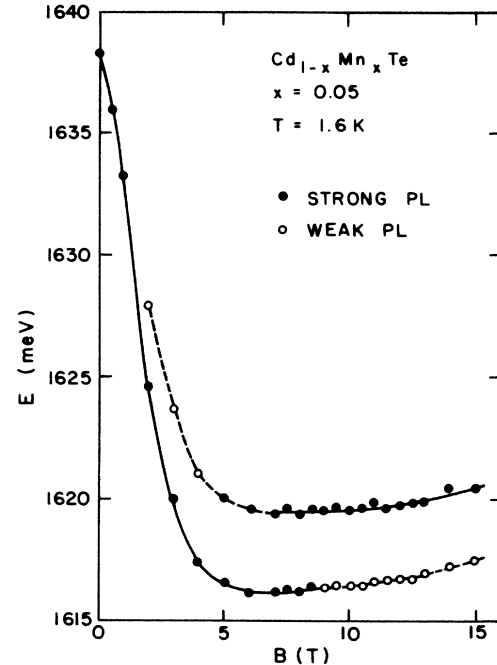
VI. CONCLUSION

Sample purity of unintentionally doped (Cd,Mn)Te was found to depend strongly on the growth technique. In the purest samples, grown by LPE and TSM, the PL was dominated by free or trapped exciton recombination and showed almost no recombination due to excitons bound to acceptor impurities or defects. On the other hand, Bridgman-grown samples had strong PL from bound excitons. Thus we expect that the concentration of impurities and native defects is largest in the Bridgman-grown samples and lowest in the LPE-grown material. The samples grown by TSM were generally much better than those grown by the Bridgman technique but not quite as pure as those grown by LPE. From changes in PL intensities we estimate that the concentrations of impurities or native defects varied by 2 orders of magnitude for different growth techniques.

We were able to determine the manganese concentration for low-x samples ($x \leq 0.3$) from the low-temperature PL spectra. This method provides an uncertainty in x of 0.002. The only difficulty with this method is in identifying the exciton PL lines ($L1$ and $L2$). Variations in the sample purity changes the relative intensities of the PL peaks and in some cases eliminates one completely. An incorrect line identification amounts to an error in x of less than 0.01.

By applying an external magnetic field, the PL from electron-hole recombination becomes polarized. At low

temperatures the polarization saturates at low fields, ~ 0.5 T, which is about an order of magnitude lower than the field at which the magnetization saturates, ~ 5 T. This is attributed to the large splitting of the bands caused by the amplified exchange field, which is larger than the external field by $\tilde{g}/g_{Mn}$ at low fields. The large splitting prohibits significant thermal population of the higher-lying state. As pointed our earlier, the polarization exists even when the inhomogeneous broadening of the bands is much larger than the splitting, such as for the PL from the donor-acceptor pair recombination band.

Observing the polarization in either Faraday or Voigt geometries gives information on spin and orbital wave-function contributions, respectively, of the recombining states. Measurements of the polarization of the DAP band in the (Cd,Mn)Se spectra indicate that the acceptor-bound hole has a large effective dipole moment of 50 Bohr magnetons at $T = 12$ K. Above $T = 12$ K the moment decreases with increasing T, where the exchange alignment is overcome by thermal dealignment. At temperatures below $T = 12$ K, the moment is dominated by the hole BMP and we suggest that the full polaron moment is limited by a spin-diffusion bottleneck.

Using the Voigt configuration for measurements of the linear polarization, we can distinguish between recombination of $m_j = \frac{1}{2}$ and $m_j = \frac{3}{2}$ hole states in the (Cd,Mn)Te spectra. The $L1$ line is only weakly polarized at larger fields and is assigned to the recombination of the $(\frac{1}{2}, \frac{3}{2})$ hole pair state of the acceptor-bound exciton. On the other hand, the $L2$ line polarizes completely at low fields indicative of recombination of a single $\frac{3}{2}$ hole state. This provides additional evidence that the $L2$ line is due to trapped excitons, as suggested by Golnik, Ginter, and Gaj.[20]

Magnetic-field-induced transitions of impurity-bound

excitons are observed in the PL spectrum of both (Cd,Mn)Te and (Cd,Mn)Se. For increasing field the two like-particles (electrons or holes) prefer to have the same spin state; however, Pauli exclusion keeps them from sharing the same orbital. Above the transition field one particle makes a transition to a large spatial orbit with an accompanying reduction in the binding energy. This reduced binding effectively releases the exciton from the impurity center (ionization). Quantitative agreement with a simple model is found for the donor-bound exciton in (Cd,Mn)Se.

Finally, we observe a step in the PL energy caused by the magnetic-field-induced transition of a pair of manganese ions. This step reflects a step in the magnetization when the pair makes a transition from the $S_1 + S_2 = 0$ ground state to the $S_1 + S_2 = 1$ first excited state. Because of background effects, the transition was only observed for the (Cd,Mn)Se spectra. The PL technique for measuring the steps is probably limited to only a few SMSC materials.

[1] N. B. Brandt and V. V. Moshchalkov, Adv. Phys. **33**, 193 (1984); J. K. Furdyna, J. Appl. Phys. **53**, 7637 (1982); and references cited therein.

[2] R. R. Galazka, in *Proceedings of the XIV International Conference on the Physics of Semiconductors, Edinburgh, 1978*, edited by B. C. H. Wilson (IOP, Bristol, 1978), p. 133.

[3] P. A. Wolff, in *Semiconductors and Semimetals*, edited by R. K. Willardson and A. C. Beer (Academic, New York, 1986).

[4] J. A. Gaj, J. Ginter, and R. R. Galazka, Phys. Status Solidi **89**, 655 (1978).

[5] A. V. Komarov, S. M. Ryabchenko, O. V. Terletskii, I. I. Zheru and R. D. Ivanchuk, Zh. Eksp. Teor. Fiz. **73**, 608 (1977) [Sov. Phys.—JETP **46**, 318 (1977)].

[6] D. Heiman, P. A. Wolff, and J. Warnock, Phys. Rev. B **27**, 4848 (1983).

[7] A. Golnik, J. A. Gaj, M. Nawrocki, R. Planel, and C. Benoit à la Guillaume, J. Phys. Soc. Jpn., Suppl. A, **49**, 819 (1980).

[8] M. Nawrocki, R. Planel, G. Fishman, and R. R. Galazka, Phys. Rev. Lett. **46**, 735 (1981).

[9] M. Ryabchenko and Yu. Semenov, Zh. Eksp. Teor. Fiz. **84**, 1419 (1983) [Sov. Phys.—JETP **57**, 825 (1983)].

[10] T. Dietl and J. Spalek, Phys. Rev. B **28**, 1548 (1983).

[11] R. Planel, J. Gaj, and C. Benoit à la Guillaume, J. Phys. (Paris) C **5**, 39 (1980).

[12] S. M. Ryabchenko, O. V. Terlatskii, I. B. Mizetskaya, and G. S. Oleinik, Fiz. Tekh. Poluprovodn. **15**, 2314 (1981) [Sov. Phys. Semicond. **15**, 1345 (1981)].

[13] S. I. Gubarev and B. N. Shepel, Pisima Zh. Eksp. Teor. Fiz. **37**, 528 (1983) [JETP Lett. **37**, 629 (1983)].

[14] D. Heiman, Appl. Phys. Lett. **42**, 775 (1983).

[15] M. P. Vecchi, W. Giriat, and L. Videla, Appl. Phys. Lett. **36**, 99 (1981).

[16] M. M. Moriwaki, W. M. Becker, W. Gebhardt, and R. R. Galazka, Solid State Commun. **39**, 367 (1981); and W. M. Becker, R. Bylsma, M. M. Moriwaki, and R. Y. Tao, *ibid.* **49**, 245 (1984).

[17] A. Golnik, J. A. Gaj, M. Nawrocki, R. Planel, and C. Benoit à la Guillaume, J. Phys. Soc. Jpn., Suppl. C **49**, 819 (1980).

[18] T. H. Nhung, R. Planel, C. Benoit à la Guillaume, and A. K. Bhattacharjee, Phys. Rev. B **31**, 2388 (1985).

[19] D. Heiman, J. Warnock, P. A. Wolff, R. Kershaw, D. Ridgley, K. Dwight, and A. Wold, Solid State Commun. **52**, 909 (1984).

[20] A. Golnik, J. Ginter, and J. A. Gaj, J. Phys. C **16**, 6073 (1983).

[21] J. Warnock and P. A. Wolff, Phys. Rev. B **31**, 6579 (1985).

[22] J. Warnock, R. Kershaw, D. Ridgley, K. Dwight, A. Wold, and R. R. Galazka, J. Lumin. **34**, 25 (1985).

[23] J. H. Harris and A. V. Nurmikko, Phys. Rev. Lett. **51**, 1477

(1983).

[24]J. J. Zayhowski, C. Jagannath, R. N. Kershaw, D. Ridgley, K. Dwight, and A. Wold, Solid State Commun. **55**, 941 (1985).

[25]J. J. Zayhowki, Ph.D. thesis, Massachusetts Institute of Technology, 1986.

[26]B. Khazai, R. Kershaw, K. Dwight, and A. Wold, Mat. Res. Bull. **18**, 217 (1983).

[27]P. Becla (unpublished).

[28]R. Triboulet and G. Didier, J. Cryst. Growth **28**, 29 (1974).

[29]D. Heiman, Rev. Sci. Instrum. **56**, 684 (1985).

[30]A. Twardowski, M. Nawrocki, and J. Ginter, Phys. Status Solidi **96**, 497 (1979).

[31]J. Stankiewicz, N. Bottka, and W. Giriat, J. Phys. Soc. Jpn., Suppl. A **49**, 827 (1980).

[32]Y. R. Lee and A. K. Ramdas, Solid. State Commun. **51**, 861 (1984).

[33]J. Stankiewicz, Phys. Rev. B **27**, 3631 (1983).

[34]D. Heiman, Y. Shapira, S. Foner, B. Khazai, R. Kershaw, K. Dwight, and A. Wold, Phys. Rev. B **29**, 5634 (1984).

[35]R. L. Aggarwal, S. N. Jasperson, J. Stankiewicz, Y. Shapira, S. Foner, B. Khazai, and A. Wold, Phys. Rev. B **28**, 6907 (1983).

[36]A. Petrou, J. Warnock, R. N. Bicknell, N. C. Giles-Taylor,

and J. F. Schetzina, Appl. Phys. Lett. **46**, 692 (1985).

[37]C. A. Huber, A. V. Nurmikko, M. Gal, and A. Wold, Solid State Commun. **45**, 41 (1983).

[38]L. Bryja and J. A. Gaj, Acta Phys. Polon. **A67**, 303 (1985).

[39]Y. Shapira, S. Foner, D. Ridgley, K. Dwight, and A. Wold, Phys. Rev. **B30**, 4021 (1984).

[40]R. L. Aggarwal, S. N. Jasperson, Y. Shapira, S. Foner, T. Sakakibara, T. Goto, N. Miura, K. Dwight, and A. Wold, in *Proceedings of the 17th International Conference on the Physics of Semiconductors,* edited by J. D. Chadi and W. A. Harrison (Springer-Verlag, New York, 1985), p. 1419.

[41]Y. Shapira, S. Foner, P. Becla, D. N. Domingues, M. J. Naughton, and J. S. Brooks, Phys. Rev. B **33**, 356 (1986).

[42]R. L. Aggarwal, S. N. Jasperson, P. Becla, and R. R. Galazka, Phys. Rev. B **32**, 5132 (1985).

[43]N. Yamada, S. Takeyama, T. Sakakibara, T. Goto, and N. Miura, Phys. Rev. B **34**, BH3145 (1986).

[44]L. M. Corliss, J. M. Hastings, S. M. Shapiro, Y. Shapira, and P. Becla, Phys. Rev. B **33**, 608 (1986).

[45]D. Heiman, E. D. Isaccs, S. Foner, Y. Shapira, P. Becla, K. Dwight, R. Kershaw, and A. Wold (unpublished).

[46]D. Seiler, D. Heiman, R. Feigenblatt, R. L. Aggarwal, and B. Lax, Phys. Rev. B **25**, 7666 (1982).